SHOCK, Vol. 51, No. 2, pp. 228–234, 2019

CEREBRAL MULTIMODAL MONITORING IN SEPSIS: AN EXPERIMENTAL STUDY

Pedro Kurtz, Joana C. d'Avila, Darwin Prado, Caroline Madeira, Charles Vargas-Lopes, Rogerio Panizzutti, Luciano C.P. Azevedo, and Fernando A. Bozza

National Institute of Infectology, Oswado Cruz Foundation and D'Or Institute for Research and Education (IDOR), Rio de Janeiro, Brazil

Received 4 Dec 2017; first review completed 20 Dec 2017; accepted in final form 14 Mar 2018

ABSTRACT—Acute brain dysfunction is a complication of sepsis, and its pathophysiology remains poorly understood. We studied the brain metabolism in a resuscitated animal model of sepsis. Twelve anesthetized, mechanically ventilated, and invasively monitored pigs were allocated to a sham procedure (N = 5) or sepsis (N = 7). Sepsis was induced through fecal inoculation in the peritoneum. Fluid resuscitation was maintained during the entire study period. Animals were observed until spontaneous death or for a maximum of 24 h. In addition to global hemodynamic and laboratory assessment, intracranial pressure and cerebral microdialysis (MD) were evaluated at baseline, 6, 12, 18, and 24 h after sepsis induction. After euthanasia, the brain was rapidly removed and a fragment from the frontal cortex was analyzed for markers of neuroinflammation, metabolism, and neurotransmission. Septic animals developed a hyperdynamic state associated with increased arterial lactate. Cerebral microdialysis showed unchanged levels of lactate/pyruvate ratios and brain glucose between the groups. Brain/serum glucose ratios were increased in the septic animals during the study period despite a progressive decrease in serum glucose. Moreover, extracellular glutamine levels were elevated starting at 6 h after sepsis. Tissue analysis showed elevated glutamate, glutamine, and glutamine synthetase in the sepsis group. However, C-Fos, a marker of neuronal activity, was unchanged between groups. In this animal model of resuscitated sepsis, we found increased oxidative stress and alterations in neuroenergetics characterized by exacerbated activity of the glutamate/glutamine cycle and increased glucose utilization by the brain, however without any evidence of decompensated energy metabolism.

KEYWORDS—Acute brain dysfunction, cerebral multimodality monitoring, sepsis-associated encephalopathy

INTRODUCTION

Brain dysfunction is a major complication of sepsis, characterized by a spectrum of impaired consciousness, ranging from mild delirium to coma. It occurs early during sepsis and may be associated with brainstem dysfunction, electroencephalographic changes (1) and neuroimaging findings (2). Delirium is associated to increased mortality (3), and acute brain dysfunction is related to long-term cognitive impairments (4).

The pathophysiology of brain dysfunction in sepsis remains unclear. It has been linked to cellular damage, neuroinflammation, mitochondrial dysfunction, altered cerebral blood flow, and neurotransmission (5). Neurotransmission and ionic homeostasis account for most of brain energy expenditure, and most of this expenditure is related to the glutamate/glutamine cycle. Glutamate is the major excitatory amino acid, and its extracellular levels must be tightly regulated to maintain brain tissue homeostasis. Activated microglia in sepsis leads to secretion of cytokines and increased glutamate production, resulting in increased metabolic demand. Moreover, neurotransmitter reuptake, antioxidant defense, and energy substrate delivery depend on a strong metabolic cooperation between astrocytes and neurons, and these processes critically depend on energy metabolism (6). Thus, neuroinflammation and increased excitatory glutamatergic neurotransmission may lead to a bioenergetic crisis and brain dysfunction. These processes have been suggested as potential therapeutic targets in sepsis-associated encephalopathy (7, 8).

Data on nonresuscitated animal models of septic shock have shown that neuroinflammation, altered brain energy metabolism, and potentially ischemia are involved in the development of acute brain dysfunction and cognitive impairment (9–11). However, these changes were associated with refractory hypotension and tissue hypoxia, which are often absent in early sepsis-associated brain dysfunction.

Multimodal monitoring with cerebral microdialysis allows the evaluation of the extracellular neurochemical profile of the brain after sepsis induction. Coupled with tissue analysis of metabolites related to energy metabolism and neuronal function, there is opportunity to describe the potential mechanisms implicated in the development of acute brain dysfunction after sepsis.

Address reprint requests to Fernando A. Bozza, MD, PhD, Instituto Nacional de Infectologia, Fundação Oswado Cruz and Instituto D'Or de Ensino e Pesquisa, Rio de Janeiro, Brazil. E-mail: bozza.fernando@gmail.com; Co-correspondence: Pedro Kurtz, MD, PhD, Paulo Niemeyer State Brain Institute, Rio de Janeiro, Rio de Janeiro Brazil. E-mail: kurtzpedro@mac.com.

LCPA and FAB equally contributed to this work.

This work was supported by unrestricted grants from Brazilian Council for Scientific and Technological Development, Fundação Carlos Chagas Filho de Amparo a Pesquisa do Estado do Rio de Janeiro and Research and Education Institute Hospital Sirio-Libanes.

Authors' contributions: PK was responsible for conception, experimental design, data acquisition, and interpretation; JCA, DP, CM, CVL, and RP were responsible for the acquisition of data and data interpretation; LCPA was responsible for conception, experimental design, data acquisition, and interpretation; FAB was responsible for conception, experimental design, and data interpretation. All authors were responsible for drafting the article or revising it critically for important intellectual content and for final approval of the version. All authors read and approved the final manuscript.

The authors report no conflicts of interest.

Ethics approval: The study protocol was approved by the Institutional Animal Research Ethics Committee at Hospital Sirio-Libanes and was performed according to National Institute of Health guidelines for the use of experimental animals.

DOI: 10.1097/SHK.0000000000001138

The aim of this study was to evaluate the relationship of disturbances of brain metabolism and markers of neuronal function with systemic and brain hemodynamics in a large animal model of resuscitated sepsis. We hypothesized that brain metabolism and neuronal function are impaired during sepsis and that these changes are unrelated to severe hemodynamic compromise.

MATERIALS AND METHODS

The study protocol was approved by the Institutional Animal Research Ethics Committee at Hospital Sirio-Libanes and was performed according to National Institute of Health guidelines for the use of experimental animals. Instrumentation, surgical preparation, and induction of sepsis were performed as previously described (12).

Experimental animals, design, and surgical preparation

Twelve male pigs weighing approximately 40 kg were fasted for 18 h with free access to water before the experiment. The animals were premedicated with intramuscular midazolam (0.3 mg/kg) and acepromazine (0.5 mg/kg), intubated, and connected to a mechanical ventilator (Evita XL, Drager Medical, Lubeck, Germany) with a positive end expiratory pressure (PEEP) of 5 cmH_2O, oxygen inspiratory fraction (FIO_2) of 30%, tidal volume of 8 mL/kg, and respiratory rate adjusted to maintain a $PaCO_2$ value between 35 and 45 mmHg.

An introducer was placed through the external jugular vein using surgical dissection or ultrasound-guided insertion and a 7F pulmonary artery catheter (Edwards Lifesciences) was advanced into the pulmonary artery for continuous measurement of cardiac output, venous oxygen saturation, and end-diastolic volume of the right ventricle. The right femoral artery and femoral vein were surgically exposed. A 6F arterial catheter was invasively introduced into the femoral artery and connected to a pressure transducer zeroed at the mid-chest level. A double-lumen catheter was inserted through the femoral vein for drug infusion.

All animals were sedated with continuous intravenous infusions of midazolam (0.3 mg/kg/h) and fentanyl (10 mcg/kg/h), and paralyzed with a bolus (0.15 mg/kg) and a continuous infusion of pancuronium (0.25 mg/kg/h).

A midline laparotomy (approximately 4 cm) was performed in all animals. A catheter was surgically inserted in the bladder to record urinary output throughout the experiment. After a 2 cm incision in the descendent colon, 0.5 g/kg body weight of feces was collected. The colon was then sutured and returned to the abdominal cavity. Two large plastic tubes were inserted into the peritoneal cavity through the abdominal wall, one in each side, for later injection of feces in the experimental group and saline solution in the control group. The abdominal wall was then closed in two layers and the animals were then placed in prone position.

Before induction of sepsis, a crucial incision was made to open the scalp. Bilateral craniotomy was then performed in all animals using a drill to open two holes with a diameter of approximately 0.5 cm. The dura covering the frontal lobe on the right side of the cranium was visualized and opened in a small incision. A microdialysis catheter with a 10 mm membrane (CMA 70, CMA Microdialysis, Stockholm, Sweden) was then inserted to maintain the entire membrane extension inside the brain parenchyma. The dura mater on the left frontal lobe was visualized, punctured, and an intraparenchymal fiberoptic catheter (Codman ICP monitoring system, Codman Neuro, Raynham, Mass) was then inserted to measure intracranial pressure (ICP). Both catheters were placed under sterile conditions at a depth of 1 to 1.5 cm into the brain parenchyma. A CMA 106 microdialysis perfusion pump (CMA Microdialysis) was used to perfuse the interior of the catheter with sterile artificial cerebrospinal fluid (Na 148 mmol/L, Ca 1.2 mmol/L, Mg 0.9 mmol/L, K 2.7 mmol/L, Cl− 155 mmol/L) at a rate of 0.3 μL/min.

After the surgical procedures and a period of 60 min for stabilization, the feces were mixed with 200 mL of heated saline solution and infused in the seven animals of the experimental group. The control group received 200 mL of warm saline solution. During the surgical procedure and stabilization, the animals received a continuous infusion of 1 mL/kg/min of lactate Ringer solution.

The moment immediately before fecal infusion was considered as baseline. Parameters recorded at baseline and hourly throughout the experiment included heart rate, cardiac output, arterial pressure, venous saturation, blood temperature, urinary output, peak and plateau airway pressures, PEEP, tidal volume, FiO_2, oxygen saturation, and ICP. Arterial and mixed venous blood analyses were performed at baseline every 3 h to measure glucose, arterial lactate, pH, pO_2, pCO_2, bicarbonate, base excess, hemoglobin, and hematocrit (ABL 700, Radiometer, Copenhagen, Denmark). Body surface areas, cardiac index, and cerebral perfusion pressure were calculated using standard formulas. At baseline and every 3 h ICP, CPP and microdialysis parameters (lactate, glucose, pyruvate, glutamate, glycerol) were also recorded. After injection of feces all animals received a continuous intravenous infusion of 5 mL/kg/h of lactate ringer solution. Additional boluses of crystalloids (500 mL) were administered if mean arterial pressure (MAP) declined below 65 mmHg. If the animal remained hypotensive despite volume loading, norepinephrine was initiated at a rate of 0.025 mcg/kg/min and titrated every 15 min to avoid hypotension. All animals were observed until spontaneous death or for a maximum of 24 h after the induction of peritonitis.

The animals were killed with potassium chloride overdose after anesthesia deepening. The brain was rapidly removed, immediately frozen in liquid nitrogen and stored in a freezer −80°C until processing. A small fragment of frontal cortex was removed, weighed, and diluted 10-fold in homogenization buffer contained 20 mM Tris-HCl (pH 7.4), 2 mM EDTA and a cocktail of protease inhibitors (Roche complete mini, Basel, Switzerland).

Cerebral microdialysis and tissue metabolite analysis

After the MD catheter placement, 1 h of stabilization was allowed before sampling for normalization of changes due to probe insertion. Samples were then collected every 3 h into a microvial and immediately analyzed for glucose, lactate, pyruvate, glutamate, and glycerol (mmol/L) with the CMA 600 analyzer (CMA Microdialysis). The analyzer was automatically calibrated on initiation using standard calibration solutions from the manufacturer. The remaining perfusate was frozen in a −70°C freezer for a posterior analysis.

The homogenized tissues or microdialysis samples were treated to measure amino acids levels by high performance liquid chromatography as previously described. Amino acid concentrations were expressed per gram of total proteins in tissue homogenates or micromolar concentration in microdialysis. Tissue fragments were homogenized at 4°C in RIPA buffer (Sigma, St. Louis, Mo). Total protein concentrations were determined using the BCA assay (Pierce). Equal amounts of proteins (10 g) were resolved in 4% to 15% polyacrylamide gels and transferred to PVDF (polyvinylidene difluoride) membranes. Membranes were probed with primary antibodies, followed by the appropriate secondary antibody conjugated with infrared dyes (LI-COR Biosciences). Primary antibodies used were anti-c-fos (1:500; Abcam, Cambridge, Mass), anti-Glutamine Synthetase (1:10,000, BD Biosciences), anti- 4-hydroxynonenal (1:500; Abcam) and anti-actin (1:10,000; Abcam). Immunoreactive bands were visualized and quantified using Odyssey Infrared Imaging System (LI-COR Biosciences). The relative levels of each protein were calculated as a ratio against actin, normalized to those of controls run in the same gel.

Statistical analysis

Statistical analysis was performed using IBM SPSS Statistics for Macintosh, Version 23.0 (IBM Corp Armonk, NY) and GraphPad Prism, version 6.0 for Mac OS X (GraphPad Software Inc., San Diego, Calif). Data are presented as mean ± SD or median (IQR range). Normal distribution was confirmed using the Kolmogorov–Smirnov test. Variables were compared using parametric Student *t* tests or Mann–Whitney *U* tests for nonparametric data. The significance of differences in the measured variables between groups was analyzed using a two-way (time and groups) analysis of variance (ANOVA) followed by a Bonferroni *post hoc* analysis. A P value of <0.05 was considered statistically significant.

RESULTS

Twelve animals were used, seven in the sepsis group and five in the sham group. All but one animal survived during the 24 h of the study period. This animal presented sudden cardiac arrest after 12 h of sepsis. At baseline, there were no significant differences between groups in hemodynamic and respiratory variables (Table 1). In the sepsis group, heart rate, cardiac output, and arterial lactate increased, whereas serum glucose and base excess decreased during the study period in the sepsis group, as compared with sham animals. The mean arterial pressure decreased significantly from baseline in the septic animals. Although arterial lactate increased significantly in septic animals, none developed refractory hypotension or used noradrenaline during the study period.

Table 1. **Evolution of variables over time in septic (n = 7) and sham (n = 5) animals**

Parameter	Group	Baseline	6 h	12 h	18 h	24 h	ANOVA within group	ANOVA sepsis vs. sham
Heart rate, beats/min	Sepsis	139 ± 8.9	172 ± 10	169 ± 10	158 ± 15	155 ± 13	0.2	<0.001
	Sham	108 ± 14	96 ± 10	105 ± 7	115 ± 14	106 ± 7	0.8	
Cardiac output, L/min	Sepsis	5.1 ± 0.4	6.3 ± 1.2	6.5 ± 1.4	7.5 ± 2.9	–*	0.6	0.03
	Sham	4.9 ± 0.6	4.8 ± 0.6	4.7 ± 0.5	4.6 ± 0.9	4.8 ± 0.5	0.9	
Temperature, °C	Sepsis	39.4 ± 0.6	40.8 ± 0.7	41.1 ± 0.6	41.5 ± 0.3	41.5 ± 0.3	0.07	<0.001
	Sham	36.4 ± 0.7	37.3 ± 0.7	38.5 ± 1	39.3 ± 1.3	39.8 ± 0.9	0.1	
Pulmonary artery occlusion pressure, mmHg	Sepsis	9 ± 1.2	9.8 ± 1.1	10 ± 1	10 ± 2	13 ± 3	0.4	0.24
	Sham	11.2 ± 1.4	12.6 ± 2	11 ± 1	10 ± 2	12 ± 1	0.8	
Mean arterial pressure, mmHg	Sepsis	114 ± 4.3	93 ± 4	89 ± 3	84 ± 5	76 ± 4	<0.00	<0.001
	Sham	122 ± 9.7	116 ± 13	113 ± 12	111 ± 12	108 ± 16	0.9	
Intracranial pressure, mmHg	Sepsis	13 ± 2.1	15 ± 2	15 ± 2	16 ± 1	16 ± 0.6	0.9	0.8
	Sham	10 ± 4.1	13 ± 3	13 ± 4	17 ± 6	18 ± 5	0.6	
Cerebral perfusion pressure, mmHg	Sepsis	101 ± 3.6	78 ± 2	75 ± 2	71 ± 5	62 ± 4	<0.00	0.001
	Sham	112 ± 13	102 ± 15	100 ± 15	93 ± 21	96 ± 25	0.8	
Oxygen delivery, mL	Sepsis	709 ± 57	1045 ± 233	809 ± 193	–*	–*	0.5	0.2
	Sham	655 ± 113	599 ± 134	585 ± 91	535 ± 171	619 ± 97	0.9	
P/F ratio	Sepsis	350 ± 20	350 ± 19	352 ± 22	335 ± 29	–†	0.9	0.8
	Sham	386 ± 44	348 ± 37	341 ± 31	322 ± 34	319 ± 33	0.7	
pH	Sepsis	7.5 ± 0.02	7.45 ± 0.0	7.4 ± 0.1	7.5 ± 0.0	7.5 ± 0.0	0.8	0.1
	Sham	7.5 ± 0.05	7.5 ± 0.0	7.5 ± 0.0	7.5 ± 0.0	7.5 ± 0.0	0.9	
PaO_2, mmHg	Sepsis	127 ± 6	122 ± 8	125 ± 6	120 ± 9	126 ± 16	0.9	0.2
	Sham	126 ± 6	113 ± 15	115 ± 10	109 ± 12	108 ± 12	0.8	
Base excess	Sepsis	2.6 ± 0.9	0.8 ± 0.9	-3.8 ± 4	1.2 ± 0.3	-1 ± 0.3	0.1	<0.001
	Sham	4.9 ± 1	4.4 ± 0.7	4.5 ± 1.3	3.7 ± 1.6	5.9 ± 1	0.7	
Lactate, mg/dL	Sepsis	10.8 ± 1.2	14.9 ± 1.4	20 ± 7	18 ± 2	28 ± 13	0.2	0.048
	Sham	11.8 ± 1.7	14.8 ± 2.8	15 ± 2	13 ± 8	12 ± 4	0.8	
Hemoglobin, g/dL	Sepsis	10.5 ± 0.4	12.8 ± 0.8	11.2 ± 0.5	11 ± 1	9.2 ± 0.1	0.06	0.02
	Sham	9.8 ± 0.6	10.1 ± 0.8	9.6 ± 0.8	8.6 ± 0.7	10.2 ± 1.3	0.7	
Glucose, mg/dL	Sepsis	115 ± 12	75 ± 4	64 ± 3	53 ± 2	48 ± 11	<0.00	<0.001
	Sham	130 ± 22	120 ± 6	107 ± 6	94 ± 8	90 ± 5	0.9	
SvO_2, %	Sepsis	59 ± 3	55 ± 0.9	51 ± 2	52 ± 3	51 ± 6	0.2	0.2
	Sham	71 ± 3	55 ± 13	61 ± 5	56 ± 5	–†	0.4	
Plateau pressure, mmHg	Sepsis	17.4 ± 2.6	17 ± 2	18 ± 1	19 ± 2	23 ± 3	0.4	0.9
	Sham	18 ± 1.7	19 ± 2	19 ± 2	20 ± 2	20 ± 2	0.9	
CaO_2, mmHg	Sepsis	139 ± 6	167 ± 12	149 ± 8	142 ± 12	121 ± 0.7	0.1	0.001
	Sham	130 ± 8	119 ± 14	121 ± 10	106 ± 10	123 ± 12	0.6	
Fluid, cumulative, mL	Sepsis	1429 ± 71	2886 ± 91	4164 ± 151	5375 ± 174	6725 ± 196	<0.00	<0.001
	Sham	1070 ± 54	2250 ± 45	3610 ± 209	4770 ± 231	5930 ± 258	<0.00	
Urine output cumulative, mL	Sepsis	0	471 ± 72	685 ± 123	1135 ± 133	1467 ± 124	<0.00	0.15
	Sham	0	704 ± 199	1015 ± 311	1281 ± 332	1603 ± 322	0.2	

Data are shown as mean ± standard deviation.
*Thermodilution-derived cardiac output data not available due to significant hyperthermia (temperature >41°C) in the sepsis group.
†Gas analysis data not available due to malfunction of the analyzer.

Cerebral microdialysis showed unchanged lactate/pyruvate ratio in both groups (Fig. 1, A and B). Brain glucose was similar between groups during the study period but the brain/serum glucose ratio was higher after 6 h of sepsis and until the end of the study period in the sepsis group as compared with sham (Fig. 1, C and D). Glutamate and glutamine were also evaluated in the extracellular space by microdialysis. Extracellular glutamine was markedly elevated in the sepsis group, whereas MD glutamate did not change during the study period or between groups (Fig. 1, E and F). Thus, the extracellular profile of the brain during the study period indicated a preserved metabolic function with potentially increased glutamate-glutamine cycle, with efficiently controlled extracellular levels of glutamate.

The analysis of the brain tissue demonstrated significant increase of glutamate and glutamine in the septic group (Fig. 2). Average 4-HNE levels were also increased in the septic group indicating the presence of oxidative stress in the tissue (Fig. 3). Moreover, tissue levels of the enzyme glutamine-synthetase were also elevated in sepsis as compared to control (Fig. 4). Together with findings of similar levels of c-Fos in the two groups, there is evidence of increased activity of the glutamate/glutamine cycle with unchanged neuronal activity (Fig. 5).

DISCUSSION

In this study, we used an experimental model of sepsis to describe the effects of severe peritonitis in brain metabolism. The key finding of this study was that sepsis is associated with increased activity of the glutamate/glutamine cycle and increased glucose utilization by the brain. However, we could not identify presence of decompensate energy metabolism or excessive neuronal activity.

In our study we used a swine model of fluid-resuscitated sepsis. Despite interspecies differences of sepsis development and brain injury between swines and humans, similarities in inflammatory profiles and responses have been shown (13). This model has also been shown to induce marked hemodynamic and systemic inflammatory alterations (14). Different

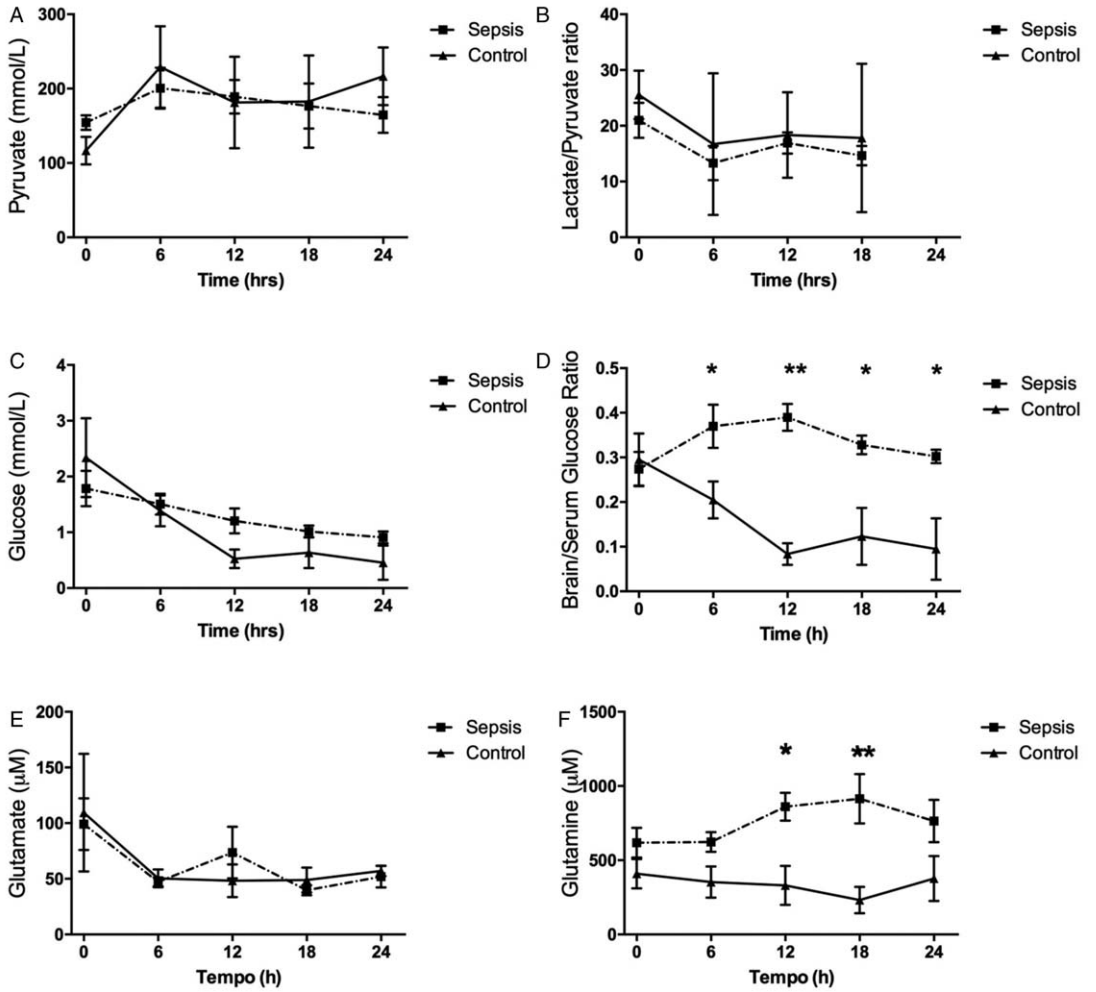

FIG. 1. **Cerebral microdialysis showing evolution in extracellular pyruvate (A), lactate/pyruvate ratio (LPR, B), glucose (C), brain/serum glucose ratio (D), glutamate (E), and glutamine (F) in the septic (n = 7, square) and sham (n = 5, triangle) animals.** Data are presented as mean ± SD. Analysis of variance (ANOVA) for brain/serum glucose ratio: $P < 0.001$ and ANOVA for glutamine: $P < 0.001$. P value of <0.05 vs. sham is represented by * and P value of <0.001 is represented by **, with *post hoc* Bonferroni correction. ANOVA was nonsignificant for cerebral pyruvate, LPR, glucose, and glutamate.

than previous studies from our group and others (10, 14, 15), the animals in the present investigation did not evolve with shock, what may be due to the fluid resuscitation or the amount of septic stimuli. This allowed us to investigate early changes in brain function in the absence of severe hypotension. Septic animals developed a hyperdynamic state with tachycardia and increased cardiac output, with a relative reduction of mean arterial pressure and cerebral perfusion pressure. Increased arterial lactate levels further reinforce the severity of sepsis. However, animals in either group had altered base excess levels, PaO_2/FiO_2 ratios or refractory hypotension suggesting our model did not reflect severe septic shock states.

Cerebral multimodal monitoring with microdialysis and brain oxygenation has recently been studied in combination with microcirculation in animal models of sepsis (10, 15). Although microdialysis allows for intermittent analysis of brain

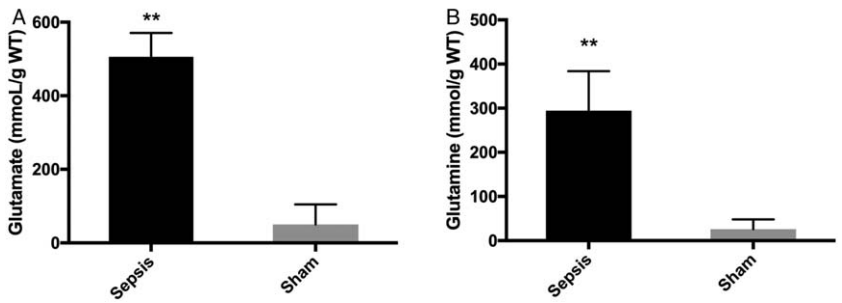

FIG. 2. **Markers of glutamatergic neurotransmission in the frontal cortex of animals with sepsis. Brain tissue was obtained after 24 h of sepsis onset or after death.** Effects of sepsis on glutamate (A) and glutamine (B). The statistical significance is expressed as $^{*}P < 0.05$ and $^{**}P < 0.001$; n = 7 (sepsis) and n = 5 (sham).

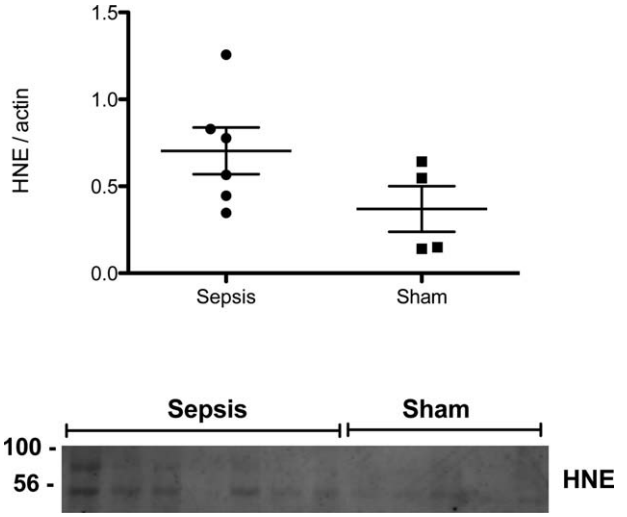

FIG. 3. **Oxidative stress in the frontal cortex of animals with sepsis.** Oxidative stress was assessed by western blotting for 4-hydroxynonenal, a product of lipid peroxidation that binds covalently to proteins used as marker of tissue oxidative damage. Optical density of the immunoreactive bands were quantified and expressed as a ration against actin, used as a loading control of the assay.

tissue, it should be stressed that its evaluation is limited to extracellular levels of metabolites in a limited focal area. Results showed that, although cortical microcirculatory impairment occurred earlier, brain metabolic distress (high LPR) and tissue hypoxia (low PbtO2) developed mostly during shock. The authors suggested that refractory hypotension and, potentially, cerebral hypoperfusion are critical factors in the development of anaerobic metabolism in the septic brain (10). Acute brain dysfunction, however, develops early and independent of hypotension in patients with sepsis (3). Our results demonstrated that, in the absence of overt shock, brain energy metabolism seems to be compensated. Although extracellular LPR and glucose are similar in the two groups, the brain/serum glucose ratios differ. This finding indicates that compensatory mechanisms, such as increased glucose uptake, must be underway to maintain metabolic balance. FDG-PET data on brain glucose metabolism in sepsis show conflicting results. When PET was performed in a mice model of sepsis induced by LPS, glucose uptake was reduced in some areas of the brain and preserved in others (16). These findings were concomitant with neuroinflammation and reduced cerebral blood flow. However, the study findings are limited by the low severity of LPS-induced systemic changes of the septic animals. In contrast, more recent data show convincing evidence that glucose uptake is increased in the brain during sepsis. This is also in accordance with findings that suggest that glycolytic pathways are activated in neuroinflammation (17, 18). The increased uptake of glucose by the brain may explain similar brain glucose and LPR levels found in septic animals in the presence of lower systemic glucose.

In addition to compensated parameters of brain metabolism, cerebral microdialysis showed unchanged levels of glutamate and elevated levels of glutamine starting after 6 h of sepsis induction. In a similar model of sepsis, high extracellular glutamate only developed with mean arterial pressure lower than 65 mmHg, suggesting ischemia as the main determinant (10). As the major neurotransmitter of the brain, glutamate is intimately related to its energy metabolism, comprising up to 80% of synaptic input. The glutamate–glutamine cycle comprises the transfer of glutamate from neurons to astrocytes and the corresponding return of glutamine from astrocytes to neurons (19). Glutamine synthetase converts glutamate, taken up from the synaptic cleft, to glutamine in an ATP-dependent process (20) undergone in the astrocyte (7, 21) (Fig. 6). Our findings of increased extracellular glutamine with unchanged extracellular glutamate may be interpreted as an exacerbated glutamate–glutamine cycle, with preserved and tightly regulated mechanisms of glutamate uptake (7).

In line with the hypotheses that this cycle is exacerbated in septic animals, analyses of brain tissue homogenates showed elevated levels of glutamate and glutamine (Fig. 2), as well as increased levels of glutamine synthetase (Fig. 4). Glutamate production can result from uptake and recycle as well as be stimulated by neuroinflammation (6). Increased glutamine synthetase activity has been shown to be protective in experimental models of stroke and its inhibition enhances release of inflammatory mediators of LPS-activated microglia (7, 21). Our concomitant findings of increased glutamate–glutamine cycle and somewhat higher 4-HNE levels could indicate an exacerbated excitatory neurotransmission, potentially excitotoxicity, associated with brain oxidative stress (11). However, c-Fos levels were unchanged in the brain tissue of septic and sham animals (Fig. 5). One potential explanation for the presence of increased glutamate–glutamine cycle with unaltered neurotransmission would be a global synaptic deficit observed in experimental sepsis (22). This reduction is probably a consequence of microglia activation and production of IL-1β and may be an underlying mechanism related to acute brain dysfunction and cognitive impairment after sepsis. Increased glutamine synthetase activity may also play a protective role avoiding harmful glutamate levels in the extracellular space and consequent excitotoxicity. We also observed signs of brain

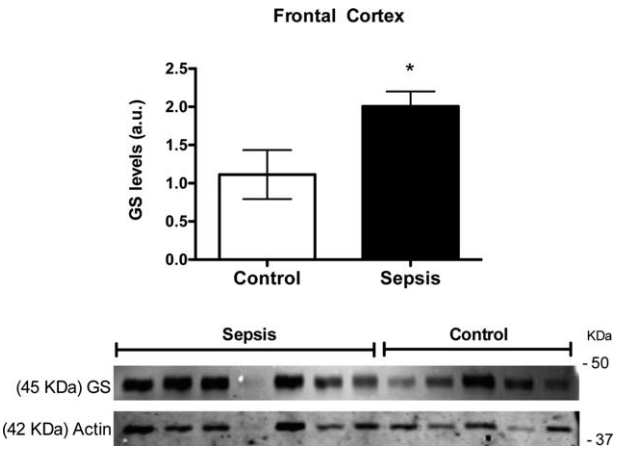

FIG. 4. **Glutamine synthetase expression is increased in the frontal cortex of animals with sepsis.** Quantitative immunoblotting for glutamine synthetase (GS) in brain tissue of the frontal cortex of the animals. GS levels are expressed as GS bands intensity normalized by actin bands intensity. Unpaired *t* test statistical significance expressed as $^{*}P < 0.05$; N = 6 (sepsis) and N = 4 (sham). Results represent the mean ± SD.

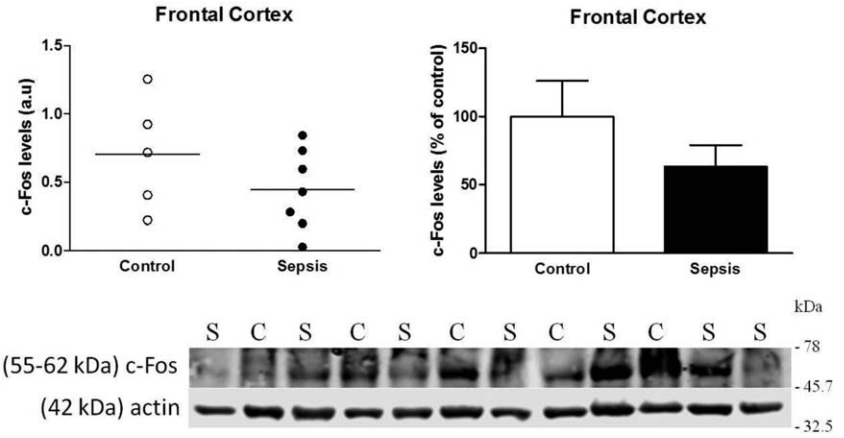

FIG. 5. **Markers of excitotoxicity.** Immunodetection (western blotting) for c-Fos (and actin) in brain tissue of the frontal cortex of the animals.

oxidative stress as shown by the increased content of brain 4-HNE in the septic animals (Fig. 3). It has been shown in different experimental models of sepsis that early oxidative stress, a molecular marker of inflammation in sepsis, is associated with innumerous neuropathologies and with cognitive impairment in survivors (11, 23).

Glutamate has an essential role in the neurometabolic coupling of the brain by acting on astrocytes. Although it has not been shown in sepsis, increased glutamatergic activity produces a shift of glucose utilization toward astrocytes (24) and triggers aerobic glycolysis as a mean to produce energy and provide substrates, such as pyruvate and lactate, to neurons, where they are oxidized to produce ATP (6). Glutamate, however, is mainly converted to glutamine by glutamine synthetase at the expense of 1 ATP. This cycle allows a large proportion of glutamate to be recycled to neuronal terminals to replenish the glutamate vesicular pool (19, 25, 26), what puts an energetic burden on astrocytes, resulting in a decrease in ATP content. These higher metabolic demand and energy requirements, in the context of sepsis, may lead to increased vulnerability. In this setting, oxidative stress, mitochondrial dysfunction, and decreased ATP synthesis (9, 11) may lead to neuroenergetic failure and acute brain dysfunction (5).

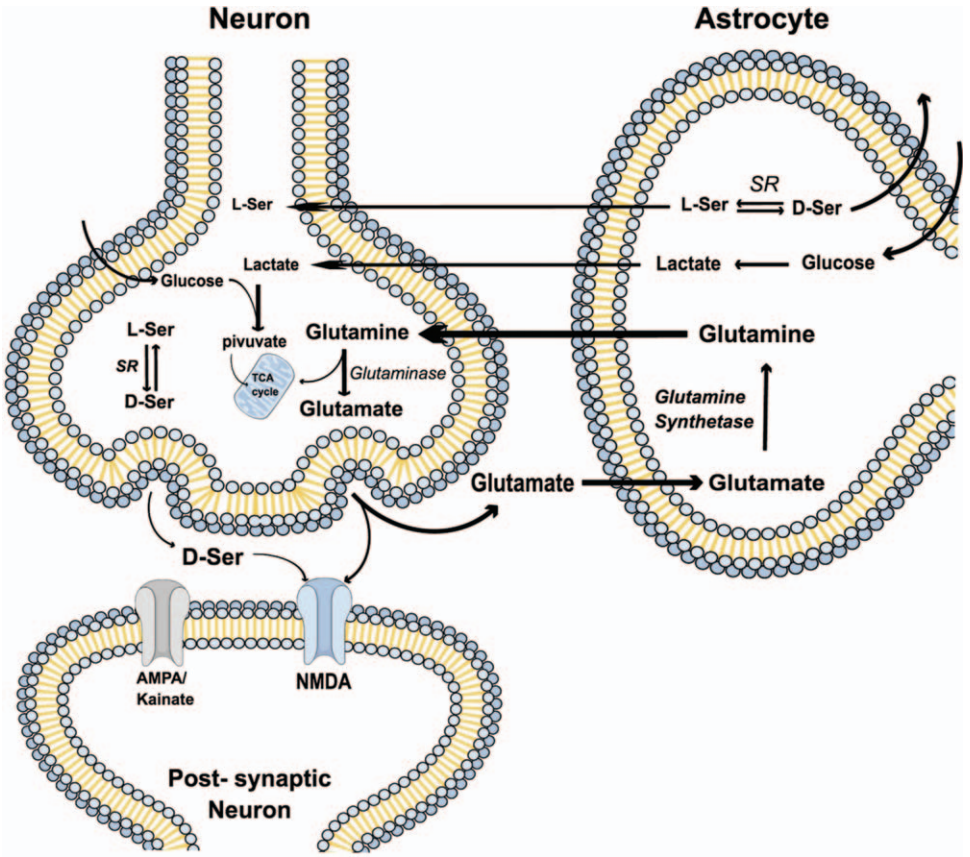

FIG. 6. **Summary of the main findings.** This figure highlights the involvement of glutamate and D-serine as coagonists of the *N*-methyl-D-aspartate receptor (NMDAr) in the process of excitotoxicity related to sepsis-associated encephalopathy. Glutamate and glutamine concentrations are increased in the brain tissue of septic animals suggesting increased glutamatergic activity.

Our findings, although preliminary, may have clinical implications. The compensated brain metabolism in our study, demonstrated by normal LPR and brain glucose in the absence of significant hypotension, reinforces the potential role of brain perfusion in the development of acute brain dysfunction, whose markers include metabolic distress and brain tissue hypoxia during septic shock. Combined with findings of microcirculatory impairment and altered cerebral autoregulation, it is likely that systemic hemodynamics has an impact on sepsis-associated brain dysfunction. Thus, depending on autoregulatory status, individualized mean arterial pressure targets could prevent brain hypoperfusion and mitigate brain dysfunction. As invasive brain monitoring cannot be advocated in patients with sepsis, clinical studies should evaluate noninvasive biomarkers of brain dysfunction, such as the impact of EEG changes, transcranial Doppler, and tissue oximetry on functional outcomes.

Our study has some limitations. First, the comparison between our model and early clinical sepsis may be partially limited because fluid resuscitation started at induction of sepsis and the animals were not treated with antibiotics. However, this design allowed us to study the impact of sepsis without the effects of hypotension on the brain. Second, our study was not randomized. To minimize bias, we alternated inclusion of animals in the sepsis and control groups. Third, we did not assess important parameters of brain function, such as EEG, tissue oxygenation, or regional blood flow. Thus, we cannot extrapolate the impact of our findings on these variables. Fourth, the surgical procedure and anesthesia induction may impact the brain's inflammatory response and sedatives/opiates have been associated with acute brain dysfunction in sepsis. However, we demonstrated significant differences between the sepsis and sham group. Fifth, for surgical and technical reasons we were not able to study intact tissue from sites of the brain other than the cortex. It is well described that the hippocampus may be more vulnerable to oxidative stress and inflammation than the cortex. Finally, animals were observed for a maximum period of 24 h which limited our conclusions about the development of later changes in brain function and longer term consequences of sepsis.

CONCLUSIONS

In this animal model of resuscitated sepsis, we demonstrate increased oxidative stress and alterations in neuroenergetics characterized by exacerbated activity of the glutamate/glutamine cycle and increased glucose utilization by the brain, however without any evidence of decompensated energy metabolism.

ACKNOWLEDGMENTS

The authors thank support from the Brazilian Council for Scientific and Technological Development, Fundação Carlos Chagas Filho de Amparo a Pesquisa do Estado do Rio de Janeiro and Research and Education Institute Hospital Sirio-Libanes.

REFERENCES

1. Azabou E, Magalhaes E, Braconnier A, Yahiaoui L, Moneger G, Heming N, Annane D, Mantz J, Chretien F, Durand MC, et al.: Early Standard Electroencephalogram Abnormalities Predict Mortality in Septic Intensive Care Unit Patients. *PLoS One* 10:e0139969, 2015.
2. Polito A, Eischwald F, Maho AL, Polito A, Azabou E, Annane D, Chretien F, Stevens RD, Carlier R, Sharshar T: Pattern of brain injury in the acute setting of human septic shock. *Crit Care* 17:R204, 2013.
3. Ely EW, Shintani A, Truman B, Speroff T, Gordon SM, Harrell FE Jr, Inouye SK, Bernard GR, Dittus RS: Delirium as a predictor of mortality in mechanically ventilated patients in the intensive care unit. *JAMA* 291:1753–1762, 2004.
4. Iwashyna TJ, Ely EW, Smith DM, Langa KM: Long-term cognitive impairment and functional disability among survivors of severe sepsis. *JAMA* 304:1787–1794, 2010.
5. Bozza FA, D'Avila JC, Ritter C, Sonneville R, Sharshar T, Dal-Pizzol F: Bioenergetics, mitochondrial dysfunction, and oxidative stress in the pathophysiology of septic encephalopathy. *Shock* 39(Suppl 1):10–16, 2013.
6. Magistretti PJ, Allaman I: A cellular perspective on brain energy metabolism and functional imaging. *Neuron* 86:883–901, 2015.
7. Palmieri EM, Menga A, Lebrun A, Hooper DC, Butterfield DA, Mazzone M, Castegna A: Blockade of Glutamine Synthetase Enhances Inflammatory Response in Microglial Cells. *Antioxid Redox Signal* 26:351–363, 2017.
8. Toklu HZ, Uysal MK, Kabasakal L, Sirvanci S, Ercan F, Kaya M: The effects of riluzole on neurological, brain biochemical, and histological changes in early and late term of sepsis in rats. *J Surg Res* 152:238–248, 2009.
9. d'Avila JC, Santiago AP, Amancio RT, Galina A, Oliveira MF, Bozza FA: Sepsis induces brain mitochondrial dysfunction. *Crit Care Med* 36:1925–1932, 2008.
10. Taccone FS, Su F, De Deyne C, Abdellhai A, Pierrakos C, He X, Donadello K, Dewitte O, Vincent JL, De Backer D: Sepsis is associated with altered cerebral microcirculation and tissue hypoxia in experimental peritonitis. *Crit Care Med* 42:e114–e122, 2014.
11. Hernandes MS, D'Avila JC, Trevelin SC, Reis PA, Kinjo ER, Lopes LR, Castro-Faria-Neto HC, Cunha FQ, Britto LR, Bozza FA: The role of Nox2-derived ROS in the development of cognitive impairment after sepsis. *J Neuroinflammation* 11:36, 2014.
12. de Azevedo LC, Park M, Noritomi DT, Maciel AT, Brunialti MK, Salomao R: Characterization of an animal model of severe sepsis associated with respiratory dysfunction. *Clinics (Sao Paulo)* 62:491–498, 2007.
13. Fairbairn L, Kapetanovic R, Sester DP, Hume DA: The mononuclear phagocyte system of the pig as a model for understanding human innate immunity and disease. *J Leukoc Biol* 89:855–871, 2011.
14. Rosario AL, Park M, Brunialti MK, Mendes M, Rapozo M, Fernandes D, Salomao R, Laurindo FR, Schettino GP, Azevedo LC: SvO(2)-guided resuscitation for experimental septic shock: effects of fluid infusion and dobutamine on hemodynamics, inflammatory response, and cardiovascular oxidative stress. *Shock* 36:604–612, 2011.
15. Taccone FS, Su F, Pierrakos C, He X, James S, Dewitte O, Vincent JL, De Backer D: Cerebral microcirculation is impaired during sepsis: an experimental study. *Crit Care* 14:R140, 2010.
16. Semmler A, Hermann S, Mormann F, Weberpals M, Paxian SA, Okulla T, Schafers M, Kummer MP, Klockgether T, Heneka MT: Sepsis causes neuroinflammation and concomitant decrease of cerebral metabolism. *J Neuroinflammation* 5:38, 2008.
17. Novy J, Allenbach G, Bien CG, Guedj E, Prior JO, Rossetti AO: FDG-PET hyperactivity pattern in anti-NMDAr encephalitis. *J Neuroimmunol* 297:156–158, 2016.
18. Jurcovicova J: Glucose transport in brain—effect of inflammation. *Endocr Regul* 48:35–48, 2014.
19. McKenna MC: The glutamate-glutamine cycle is not stoichiometric: fates of glutamate in brain. *J Neurosci Res* 85:3347–3358, 2007.
20. Schousboe A, Scafidi S, Bak LK, Waagepetersen HS, McKenna MC: Glutamate metabolism in the brain focusing on astrocytes. *Adv Neurobiol* 11:13–30, 2014.
21. Jeitner TM, Battaile K, Cooper AJ: Critical evaluation of the changes in glutamine synthetase activity in models of cerebral stroke. *Neurochem Res* 40:2544–2556, 2015.
22. Moraes CA, Santos G, de Sampaio e Spohr TC, D'Avila JC, Lima FR, Benjamim CF, Bozza FA, Gomes FC: Activated microglia-induced deficits in excitatory synapses through IL-1beta: implications for cognitive impairment in sepsis. *Mol Neurobiol* 52:653–663, 2015.
23. Barichello T, Martins MR, Reinke A, Constantino LS, Machado RA, Valvassori SS, Moreira JC, Quevedo J, Dal-Pizzol F: Behavioral deficits in sepsis-surviving rats induced by cecal ligation and perforation. *Braz J Med Biol Res* 40:831–837, 2007.
24. Porras OH, Loaiza A, Barros LF: Glutamate mediates acute glucose transport inhibition in hippocampal neurons. *J Neurosci* 24:9669–9673, 2004.
25. Bak LK, Schousboe A, Sonnewald U, Waagepetersen HS: Glucose is necessary to maintain neurotransmitter homeostasis during synaptic activity in cultured glutamatergic neurons. *J Cereb Blood Flow Metab* 26:1285–1297, 2006.
26. Stobart JL, Anderson CM: Multifunctional role of astrocytes as gatekeepers of neuronal energy supply. *Front Cell Neurosci* 7:38, 2013.